GRMHD modelling and radiative transfer

The case of M 87

Gaëtan Fichet de Clairfontaine

LUTH, Observatoire de Paris

28 november 2019

l'Observatoire de Paris LUTH

Laboratoire Univers et Théories

PSL Université Paris

1 Introduction
2 Set up
3 GRMHD results
4 Application to M 87
5 Conclusion and prospects

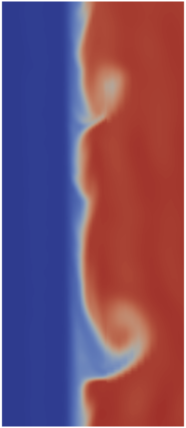

Figure: *Kelvin-Helmoltz* instabilities at the interface between the jet and the ambient medium.

Introduction

Some motivations :

- Link between the radiative process and the acceleration process in the radio band ?
- Origin of observed radio variability ? (~ month)

A plausible scenario ?

➽ Interaction of an ejecta with the structure in stationary shocks in the relativistic jet.

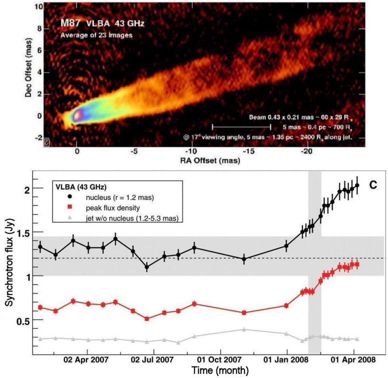

Figure: Walker et al, [2018] & Acciari et al. [2009].

Overview

GRMHD modelling and radiative transfer :

① The `MPI-AMRVAC` code [Keppens et al. (2012)] for the GRMHD simulations;

② A post-processing in `Python` to calculate the synchrotron flux component of the jet (injection and emission + relativistic effects);

➡ Extract data to form synchrotron flux map and integrate the total flux for the light curve.

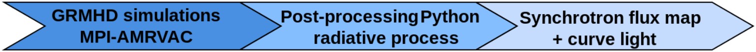

GRMHD equations :

- Resolution of the GRMHD equations for a relativistic plasma in *Minkowski* space-time;
- Numerical resolution with a conservative scheme (HLLC *Riemann* solver).

$$\partial_t\left(\Gamma\rho\right) + \nabla.\left(\rho\Gamma\mathbf{u}\right) = 0$$

$$\partial_t\left(\Gamma^2 h\mathbf{u} + \mathbf{E}\times\mathbf{B}\right) + \nabla.\left(\Gamma^2 h\mathbf{u}\mathbf{u} - \mathbf{E}\mathbf{E} - \mathbf{B}\mathbf{B} + p\,\mathbf{I}\right) = 0$$

$$\partial_t\left(h\,\Gamma^2 - p - \Gamma\rho + \frac{E^2+B^2}{2}\right) + \nabla.\left(\left(h\Gamma^2 - p - \Gamma\rho\right)\mathbf{u} + \mathbf{E}\times\mathbf{B}\right) = 0$$

$$\partial_t\mathbf{B} + \nabla.\left(\mathbf{u}\mathbf{B} - \mathbf{B}\mathbf{u}\right) = 0$$

Simulation box :

- An over-pressure inner jet allows to obtain an standing shocks structure [Hervet et al. (2017)];
- The adaptive mesh allow us to resolve more precisely certain regions.

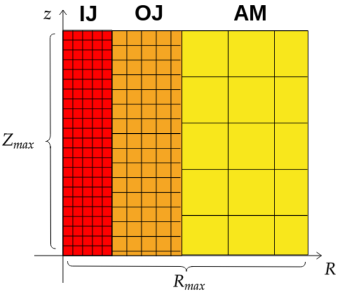

Figure: Schematic representation of the simulation box and its adaptive mesh (not at scale).

Post-processing : injection of the relativistic electrons

Power law distribution :

For each cell, we injected the relativistic electrons following [Gomez et al. (1995)] :

$$N(\Gamma)\,\mathrm{d}\Gamma = K\Gamma^{-\mathrm{p}}\mathrm{d}\Gamma$$

Valid in $\Gamma_{\mathrm{min}} < \Gamma < \Gamma_{\mathrm{max}}$ with :

$$K = \left[\frac{e_{\mathrm{th,e}}\left(\mathrm{p}-2\right)}{1-C_{\mathrm{E}}^{2-\mathrm{p}}}\right]^{\mathrm{p}-1} \left[\frac{1-C_{\mathrm{E}}^{1-\mathrm{p}}}{n_{\mathrm{e}}\left(\mathrm{p}-1\right)}\right]^{\mathrm{p}-2}$$

➡ We fixed $\Gamma_{\mathrm{min}} = 1$ and $\Gamma_{\mathrm{max}} = 10^3$: we didn't considered the cooling of the electrons.

Emissivity and self-absorption :

➤ Using approximations for the synchrotron emissivity and absorption coefficient to reduce CPU time (see Katarzyński et al. [2001])

In each cell :

- Estimation of the different parameters in the absolute frame;
- The angle θ_{obs} implies a *Doppler* beaming effect;
- × Time travel delay in the jet is not taken into account yet.

Transformation (Rybicki and Lightman [1979]) :

$$j_\nu = \delta_{\text{d}}^2 j_{\nu'} \quad : \text{ emissivity}$$

$$\alpha_\nu = \delta_{\text{d}}^{-1} \alpha_{\nu'} \quad : \text{ self-absorption}$$

$$\tau_\nu = \tau_{\nu'} \quad : \text{ optical depth}$$

$$\delta_{\text{d}} = (\Gamma(1 - \beta \cos(\theta_{\text{obs}}))^{-1}$$

Radiative transfer equation :

$$I_\nu(\tau_\nu) = \underbrace{I_\nu(0)\, e^{-\tau_\nu}}_{\texttt{i-th cell}} + \underbrace{\int_0^{\tau_\nu} \frac{j_\nu}{\alpha_\nu}\Big|_{\tau'_\nu} e^{-(\tau_\nu - \tau'_\nu)}\, d\tau'_\nu}_{\texttt{i+1-th cell}}$$

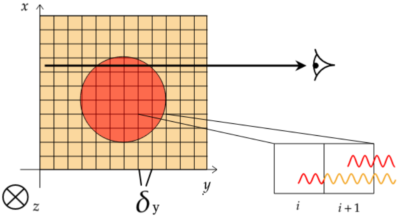

Estimation of the synchrotron flux :

$$F_\nu = \frac{S_{\mathrm{em}}}{d_l^2}(1+z)\, I_\nu$$

With the cosmological distance :

$$d_\mathrm{l} = \frac{2c}{H_0}\left(z + 1 - \sqrt{z+1}\right)$$

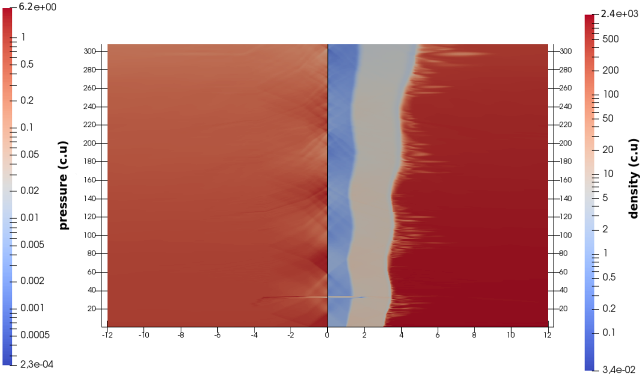

Figure: Snapshot: structured hydrodynamic jet with one ejecta. Pressure map on the left, density map on the right. Units on x- and y-axis in 0.1 pc.

Turbulent magnetic field :

We assumed : $B_{\text{turb}} = \sqrt{\dfrac{\epsilon_{\text{B}} p}{\gamma - 1}}$ with $\epsilon_{\text{B}} = 0.1$

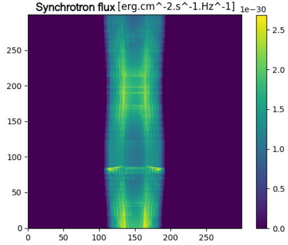

Figure: Synchrotron flux map with one ejecta with $\theta_{\text{obs}} = 90^\circ$ and $\nu = 10^9$ Hz.

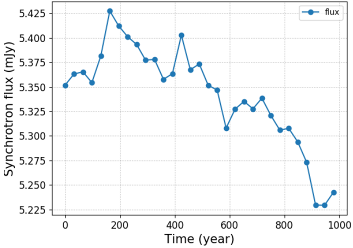

Figure: Light curve of the observed radio flux associated with the passage of an ejecta.

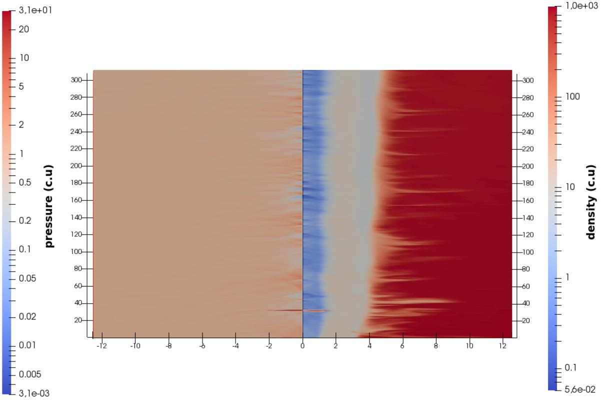

Figure: Snapshot: structured poloidal jet with an ejecta. Pressure map on the left, density map on the right. Units on x- and y-axis in 0.1 pc.

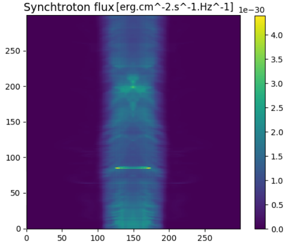

Figure: Synchrotron flux map with one ejecta with $\theta_{\text{obs}} = 90^\circ$ and $\nu = 10^9$ Hz.

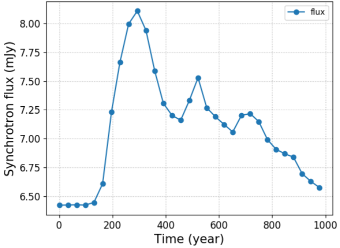

Figure: Light curve of the observed radio flux associated with the passage of an ejecta.

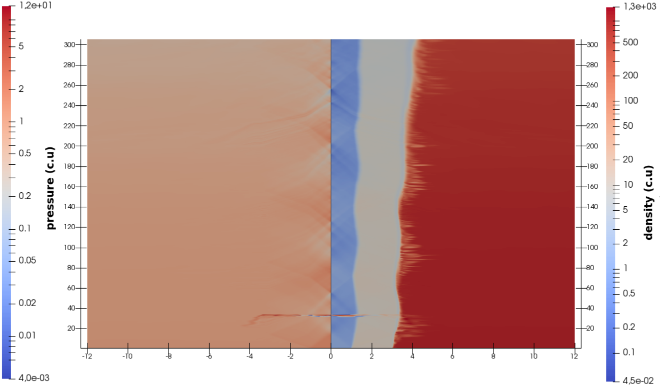

Figure: Snapshot: structured toroidal jet with an ejecta. Pressure map on the left, density map on the right. Units on x- and y-axis in 0.1 pc.

Toroidal case :

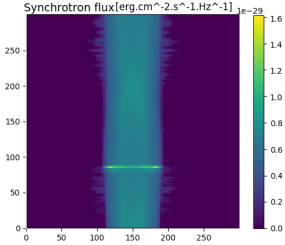

Figure: Synchrotron flux map with one ejecta with $\theta_{\text{obs}} = 90^{\circ}$ and $\nu = 10^9$ Hz.

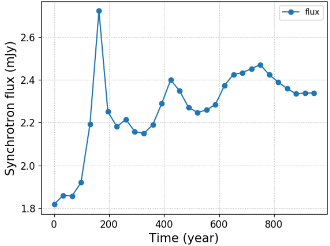

Figure: Light curve of the observed radio flux associated with the passage of an ejecta.

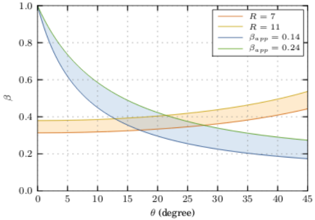

Figure: Constraint on the angle θ_{obs} (F. Mertens et al, [2016]).

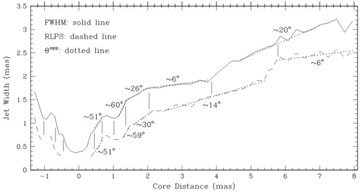

Figure: Constraint on the opening angle θ_{app} (Walker et al, [2018]).

Magnetic configuration :

We assumed a purely toroidal configuration at the base of the jet (Walker et al, [2018]).

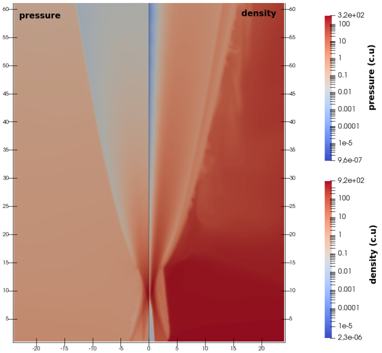

Figure: An open structured toroidal jet to simulate M 87.

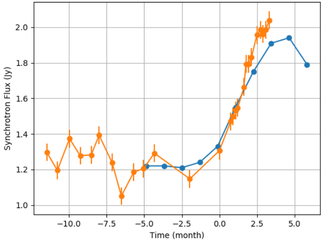

Figure: Observed radio light curve for M 87 with one ejecta in the observer frame. (orange: data from VLBA at 43 GHz; blue: our simulation).

Conclusion :

- ✗ transverse structure of the jet greatly limits the lateral energy dissipation of the ejecta;
- ✗ magnetic configuration has been found to play an important role;
- ✗ first application to a radio flare from M 87 looks promising and was the subject of a poster and a proceeding.

Prospects :

- ➡ take into account the light travel delay and the radiative loss;
- ➡ extend the model to other wavebands (X-ray, γ-ray band) to explain the other counterparts in the flare of 2008.

Thank you for your attention. Questions ?

6 More context

7 Standing and mobile shocks

8 Magnetic structure

9 Relativistic effects

10 Approximations on the synchrotron emission :

11 More on the post-processing

Gaëtan Fichet de Clairfontaine

More context

Standing and mobile shocks

Magnetic structure

Relativistic effects

Approximations on the synchrotron emission :

More on the post-processing

radio-loud AGN :

- The luminosity can reach $L_{\text{tot}} \sim 10^{47}$ erg/s;
- Non thermal emission from the radio band to the high energy gamma band;
- Multi-wavelengh observations programs.

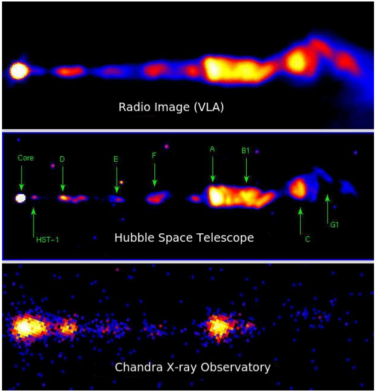

Figure: Observations map in radio / optical band (Perlman et al. [1999]) and in X band (Marshall et al. [2002]) of the M 87 jet.

Standing shocks :

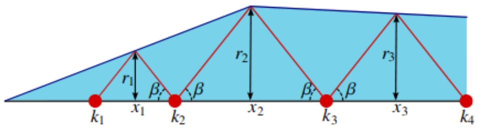

Figure: Schematic representation of the standing shocks position constraint by the radius of the jet r_n and the angle β (Hervel et al, [2017]).

Shocks structure :

- Simple recollimation shocks structure : $r_\mathrm{n} \propto k_\mathrm{n}$;
- More complex structure in the reality : in-homogeneity, external component, etc.

Standing shocks :

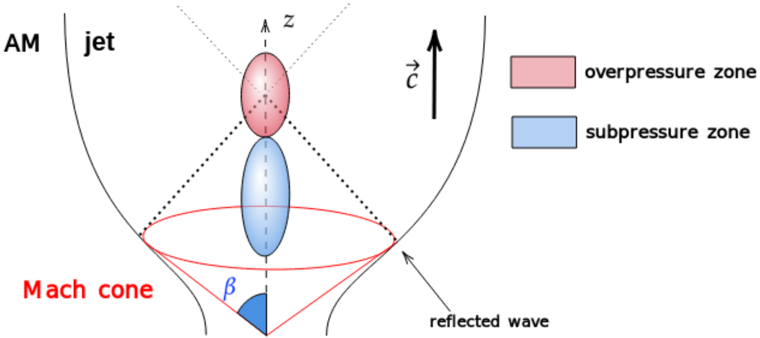

Compression wave of the ejecta :

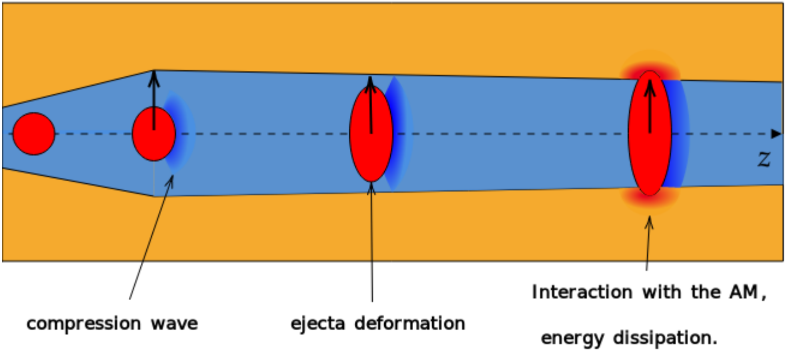

Magnetic structure influence :

- Toroidal (along φ): existence of a radial magnetic tension;
- Poloidal;
- Hydrodynamic.

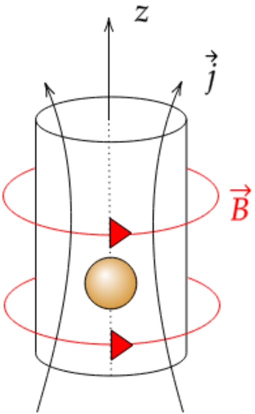

Gaëtan Fichet de Clairfontaine

More context

Standing and mobile shocks

Magnetic structure

Relativistic effects

Approximations on the synchrotron emission :

More on the post-processing

Magnetic structure influence :

- Toroidal;
- Poloidal (along z) : existence of a magnetic pressure (along r) implying a radial magnetic tension;
- Hydrodynamic.

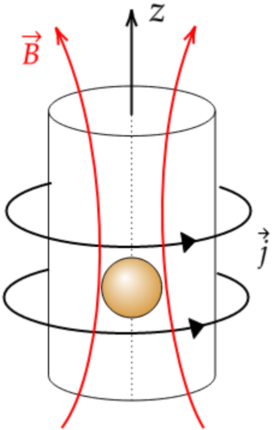

Gaëtan Fichet de Clairfontaine

More context

Standing and mobile shocks

Magnetic structure

Relativistic effects

Approximations on the synchrotron emission :

More on the post-processing

Magnetic structure influence :

- Toroidal;
- Poloidal;
- Hydrodynamic : turbulent magnetic component ?

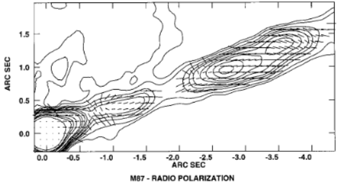

Figure: Radio polarimetry map at the base of the M 87 jet (Perlman et al, [1999]).

The other relativistic effects :

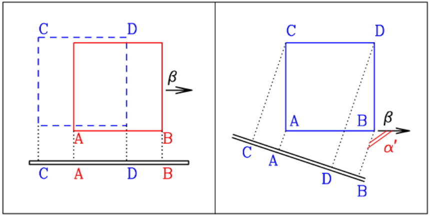

Figure: Relativistic geometric deformation of a square cell (Ghisellini [2012]).

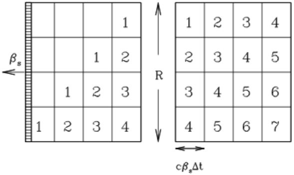

Figure: Light travel delay (Chiaberge & Ghisellini [2018]).

Assumption on P'_{syn} :

Approximation of the radiated power by an electron P'_{syn}[1](Chiaberge et al, [1999]) :

$$P'_{\text{syn}}(\nu', \Gamma) \sim \frac{3\sqrt{3}\sigma_T c U_{\text{B}}}{\pi \nu_{\text{B}}} c_1 t^{c_2} \exp(-c_3 t)$$

With :

$$U_{\text{B}} = \frac{B^2}{8\pi} \quad t = \frac{\nu'}{3\Gamma^2 \nu_{\text{B}}} \quad \nu_{\text{B}} = \frac{eB}{2\pi m_{\text{e}} c}$$

Where B is the magnetic field intensity, $c_1 = 0.78$, $c_2 = 0.25$ and $c_3 = 2.175$.

[1] This radiated power is averaged over an isotropic distribution of θ.

An example : synchrotron emissivity

We can re-write :

$$j_{\nu'}(\nu') \approx \frac{9\sigma_{\mathrm{T}} c U_{\mathrm{B}} c_1}{24\pi^2 \nu_{\mathrm{B}}} \sqrt{\frac{\nu'}{\nu_{\mathrm{B}}}} \int_{t_{\mathrm{min}}}^{t_{\mathrm{max}}} N\left(\sqrt{\frac{\nu'}{3t\nu_{\mathrm{B}}}}\right) t^{c_2-3/2} \exp(-c_3 t) \mathrm{d}t$$

Where :

$$t_{\mathrm{min}} = \frac{\nu'}{3\Gamma_{\mathrm{min}}^2 \nu_{\mathrm{B}}} \qquad t_{\mathrm{max}} = \frac{\nu'}{3\Gamma_{\mathrm{max}} \nu_{\mathrm{B}}}$$

Synchrotron emission following (Katarzynski et al, [2001]):

More context

Standing and mobile shocks

Magnetic structure

Relativistic effects

Approximation on the synchrotron emission :

More on the post-processing

$$\begin{aligned} j'_{\rm s}(\nu'_{\rm s}) &= \frac{9\sigma_{\rm T} c U_B c_1}{24\pi^2 \nu_B}\sqrt{\frac{\nu'_{\rm s}}{\nu_B}} \\ &\times \{g(\nu'_{\rm s}, t_{\rm b}, n_1, K_1) - g(\nu'_{\rm s}, t_{\rm min}, n_1, K_1) \\ &+ g(\nu'_{\rm s}, t_{\rm cut}, n_2, K_2) - g(\nu'_{\rm s}, t_{\rm b}, n_2, K_2)\} \end{aligned}$$

$$\begin{aligned} g(\nu'_{\rm s}, t, n, K) &= K\left(\frac{\nu'_{\rm s}}{3\nu_B}\right)^{\frac{-n}{2}} t^{c_2+\frac{n-1}{2}} (c_3 t)^{\frac{1-n}{2}-c_2} \\ &\times \Gamma\left(c_2 + \frac{n-1}{2}, c_3 t\right), \quad t_{\rm b} = 0 \end{aligned}$$

$$\begin{aligned} k'(\nu'_{\rm s}) &= \frac{3\sqrt{3}\sigma_{\rm T} c U_B c_1}{16\pi^2 m_{\rm e} \nu'^2_{\rm s} \nu_B} \\ &\times \{h(\nu'_{\rm s}, t_{\rm b}, n_1, K_1) - h(\nu'_{\rm s}, t_{\rm min}, n_1, K_1) \\ &+ h(\nu'_{\rm s}, t_{\rm cut}, n_2, K_2) - h(\nu'_{\rm s}, t_{\rm b}, n_2, K_2)\}, \end{aligned}$$

$$\begin{aligned} h(\nu'_{\rm s}, t, n, K) &= K(n+2)3^{\frac{n}{2}}\left(\frac{\nu'_{\rm s}}{\nu_B}\right)^{\frac{-n}{2}} t^{c_2+\frac{n}{2}} \\ &\times (c_3 t)^{-c_2-\frac{n}{2}} \Gamma\left(c_2 + \tfrac{n}{2}, c_3 t\right). \end{aligned}$$

With : $$t_{\rm min} = \frac{\nu'_{\rm s}}{3\gamma^2_{\rm min}\nu_B}, \qquad t_{\rm cut} = \frac{\nu'_{\rm s}}{3\gamma^2_{\rm cut}\nu_B}.$$

Jet power :

$$L_{\mathrm{jet}} = (\Gamma h - 1)\Gamma \rho_{\mathrm{norm}} \eta_\rho R_{\mathrm{norm}} \pi \beta c \approx \epsilon_{\mathrm{L}} \times 10^{46} \text{ erg/s}$$

Normalized quantities :

- $R_{\mathrm{norm}} \equiv 0.1$ pc
- $v_{\mathrm{norm}} \equiv c$
- $n_{\mathrm{norm}} \equiv \rho_{\mathrm{norm}} / m_{\mathrm{p}}$
- $p_{\mathrm{norm}} \equiv \rho_{\mathrm{norm}} c^2$
- $B_{\mathrm{norm}} \equiv \sqrt{8\pi p_{\mathrm{norm}}}$

→ $t_{\mathrm{norm}} = 10 \times R_{\mathrm{norm}} / c \approx 3.26$ years

Free parameters :

- ϵ_{L} : fraction of L_{jet} in the inner jet;
- η_ρ : density ratio between the inner jet and the ambient medium.

Post-processing : code units **vs** physical

Normalized quantities :

- $R_{\text{norm}} \equiv 0.1$ pc
- $v_{\text{norm}} \equiv c$
- $n_{\text{norm}} \equiv \rho_{\text{norm}} / m_{\text{p}}$
- $p_{\text{norm}} \equiv \rho_{\text{norm}} c^2$
- $B_{\text{norm}} \equiv \sqrt{8\pi \, p_{\text{norm}}}$

Physical quantities :

- $n_{\text{phys}} = n_{\text{code}} \times n_{\text{norm}}$
- $p_{\text{phys}} = p_{\text{code}} \times p_{\text{norm}}$
- $B_{\text{norm}} = B_{\text{code}} \times B_{\text{norm}}$

$\vdots$